X-ray microtomography study of the compaction process of rods under tapping

Yang Fu,[1] Yan Xi,[2] Yixin Cao,[1] and Yujie Wang[1,*]

[1]*Department of Physics, Shanghai Jiao Tong University, 800 Dong Chuan Road, Shanghai 200240, China*
[2]*School of Biomedical Engineering, Shanghai Jiao Tong University, 800 Dong Chuan Road, Shanghai 200240, China*

We present an x-ray microtomography study of the compaction process of cylindrical rods under tapping. The process is monitored by measuring the evolution of the orientational order parameter, local, and overall packing densities as a function of the tapping number for different tapping intensities. The slow relaxation dynamics of the orientational order parameter can be well fitted with a stretched-exponential law with stretching exponents ranging from 0.9 to 1.6. The corresponding relaxation time versus tapping intensity follows an Arrhenius behavior which is reminiscent of the slow dynamics in thermal glassy systems. We also investigated the boundary effect on the ordering process and found that boundary rods order faster than interior ones. In searching for the underlying mechanism of the slow dynamics, we estimated the initial random velocities of the rods under tapping and found that the ordering process is compatible with a diffusion mechanism. The average coordination number as a function of the tapping number at different tapping intensities has also been measured, which spans a range from 6 to 8.

I. INTRODUCTION

Other than having important industrial applications, understanding of the compaction process of granular materials has also attracted a lot of scientific interest recently. The close analogy of the slow dynamics displayed by granular materials under compaction with thermal glassy dynamics suggests a unifying jamming concept [1,2]. The compaction dynamics can also be used to verify possible thermodynamic descriptions of the naturally out-of-equilibrium granular systems [3]. Extensive experimental and theoretical studies have been carried out in understanding the compaction dynamics [1]: mechanisms based on free volume [4], the parking-lot model [5], etc., have been proposed; numerical simulations also offered great insight [6–8]. Phenomenologically, compaction proceeds through the filling of large voids in the packing and the reduction of free volume around a particle. As the packing gets denser, it entails the cooperative movements of an increasing number of particles and the associated relaxation time diverges exponentially [5].

Recently, there has been growing interest in using microscopic information to interpret the compaction process with the development of three-dimensional visualization techniques such as x-ray tomography [9–12]. Detailed study of particle-level dynamic [13], structural [9], and force [11] information can provide invaluable knowledge to the understanding of the compaction dynamics. In particular, it has been noted that both spatial and temporal heterogeneities have been identified as intrinsic features of granular dynamics [7,14].

Most of the past efforts on the compaction process have been focused on spherical particles [15,16]. In reality, granular particles are rarely perfectly spherical, and nonspherical particle packings have displayed many behaviors which are significantly different from their spherical counterparts. For instance, both spherocylinders and ellipsoids have maximum random packing fractions higher than the $\rho_{rcp} \approx 0.64$ limit

of spherical ones [17]. In packings made up of long rods, the rods tend to align with each other through an excluded-volume interaction [18]. Therefore, it can exhibit high degrees of ordering upon tapping under certain circumstances [19]. Nevertheless, the relaxation dynamics of nonspherical particle packings under tapping is very similar to that of spherical ones [15–18]. Therefore, the study of the compaction dynamics in nonspherical particle packings can provide different paradigms for the understanding of the universal compaction mechanism.

Different experimental laws have been proposed to interpret the macroscopic compaction dynamics. The packing density ρ of a spherical packing under tapping has been suggested by the Chicago group to follow an inverse logarithmic law [16]

$$\rho(t) = \rho_f - \frac{\rho_0 - \rho_f}{1 + B \ln(1 + t/\tau)}, \qquad (1)$$

where ρ_f and ρ_0 are the packing densities of the final and the initial states, respectively, B is a fitting constant depending on the dimensionless tapping intensity Γ, which is defined as the ratio between the measured peak acceleration and the gravitational acceleration g, and τ is the relaxation time of the exponential law with the unit of one tap. This behavior was found to be consistent with the free volume model [4].

Later studies by the Rennes group [15,20] have also found in both spherical and nonspherical packings that ρ can be well fitted with a stretched-exponential Kohlrausch-Williams-Watts law (KWW law)

$$\rho(t) = \rho_f - (\rho_f - \rho_0) \exp\left[-\left(\frac{t}{\tau}\right)^{\beta}\right], \qquad (2)$$

where β is the stretching exponent. The KWW law has usually been employed in the description of the slow dynamics in thermal glassy systems, so the close analogy of the compaction dynamics in two disparate systems implies a close connection between them. The different compaction dynamics observed by the aforementioned two groups has been attributed to the different containers used: In the Chicago group's experiment, the container was a very long tube with a small diameter

*yujiewang@sjtu.edu.cn

comparable with the particle size which prohibits convection. In the Rennes group's experiment, the container's diameter was much larger than the particle size, which significantly reduces the boundary effect. Instead, strong convection has been observed and the compaction dynamics is attributed to a convection-mediated mechanism; the corresponding relaxation time τ is suggested to be determined by the convection speed [22]. A similar stretched-exponential behavior has also been identified in studies of the compaction of two-dimensional granular particles [21,23]. However, no boundary or convection effect was observed [21,23]. Therefore, it is interesting to resolve these differences.

Due to the experimental difficulty in tracking the three-dimensional granular packing structure noninvasively, there has been a lack of experimental results on the microscopic compaction dynamics. Instead, the ordering process has been investigated primarily using macroscopic parameters such as packing density or volume fraction. Since the understanding of the compaction process using statistical mechanics ultimately requires the knowledge of distributions on the particle level, obviously, substantial information can be gained by directly investigating the microscopic structure and dynamics.

In this paper, we exploit x-ray microtomography [24] to study the compaction dynamics of a three-dimensional packing consisting of cylindrical rods under tapping. This paper is organized as follows. In Sec. II, we describe the experimental setup and the sample preparation procedure. In Sec. III, we present the behaviors of the packing density and vertical order parameter as a function of the tapping number, together with the fitting results using the KWW and the inverse logarithmic laws. We discuss the boundary effect on the ordering process in Sec. IV. In Sec. V, we discuss the Arrhenius behavior of the relaxation time as a function of tapping intensity. We also present measurements of the rods' random velocities during one tap and a possible diffusion mechanism of the slow ordering dynamics. In Sec. VI, we discuss the average coordination number of the packing as a function of the tapping number for different tapping intensities. We summarize our findings in Sec. VII.

II. EXPERIMENTAL SETUP AND PROCEDURE

We performed the experiment using uniform-sized nylon rods which are 1.0 mm in diameter and 4.0 mm in length. Each rod weighs around 3.5 mg. Approximately 350 rods were filled into a 50-mm-tall acrylic tube (10 mm inner diameter) mounted vertically on an electromagnetic exciter. The disordered packing has an initial height of ∼34 mm. The experimental setup and protocol are similar to those of Villarruel *et al.* [19] in terms of the rod size, the rod's aspect ratio, and the rod and container size ratio. The major difference lies in the much smaller filling height in our case.

A single cycle of a 30-Hz sine wave was output from a signal generator to drive the exciter, producing individual shaking or "tapping." Successive taps are spaced with 1.0 s intervals to allow the system to relax completely. In order to reduce electrostatic charges, the rods were grounded on aluminum foil before each experimental run.

The evolution of the rods' ordering process under tapping was studied by an x-ray microtomography setup (MicroXCT-200, Xradia Inc.). In our experiment, the voltage and the power of the x-ray tube were set at 40 kV and 8 W, respectively. The effective spatial resolution of the detector was 10.16 μm after optical magnification (2 $\times$). The imaging window has a field of view of 10.4 $\times$ 10.4 mm^2 and was positioned at the medium height of the packing. There are about 90 rods within the x-ray imaging window. We took 1200 projection images around the sample and the exposure time was set to 20 s for each projection image. The rods were tapped a total of 10^4 times for different Γ and tomography was conducted at several tapping numbers t for every Γ. Before each run, the container was first emptied and then refilled to form an initially disordered packing.

III. PACKING DENSITY AND ORDER PARAMETER

Figures 1(a) and 1(b) show the three-dimensional reconstructed packing structure before and after 10^4 times of tapping at $\Gamma = 3.41$, which illustrates the onset of the vertical ordering. The tomogram at the medium height of the reconstructed structure is shown in Fig. 1(c), and Fig. 1(d) is a simple image segmentation of Fig. 1(c) using a thresholding technique.

The global packing density ρ_H is calculated using the total filling height H of rods in the tube. Figure 2(a) shows the evolution of ρ_H as a function of tapping number t for different Γ. In general, ρ_H increases monotonically with t. As shown in Fig. 2(b), the maximum $\rho_H = 0.52$ can be reached at $\Gamma = 2.37$ after 10^4 times of tapping. It is noted that the final ρ_H is fairly low for all Γ investigated. This is owing to the fact that we have a small number of layers in the packing and the surface height measurements were sensitively dependent on the loosely packed surface layers. We can also directly obtain the local packing density ρ_S using the ratio between the volume occupied by the rods and the total container volume within
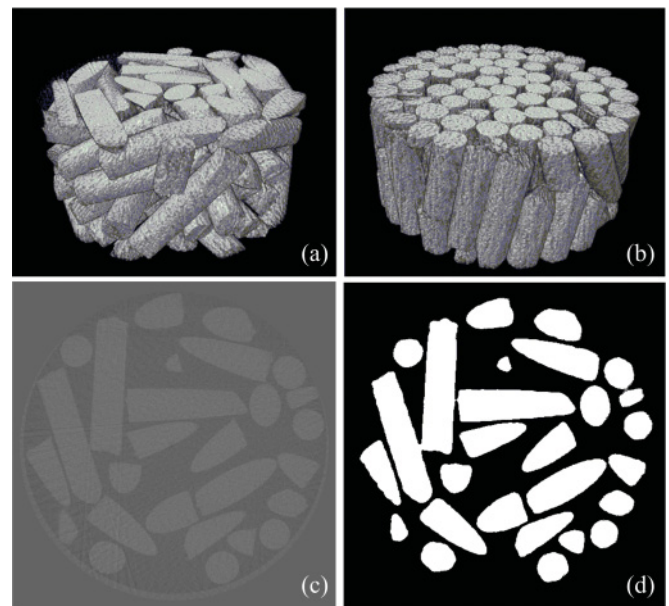

FIG. 1. X-ray tomography reconstructed rods' packing structure (a) before tapping, and (b) after 10^4 taps. (c) Tomogram at the medium height of reconstructed structure. (d) Image segmentation of (c) using simple thresholding.
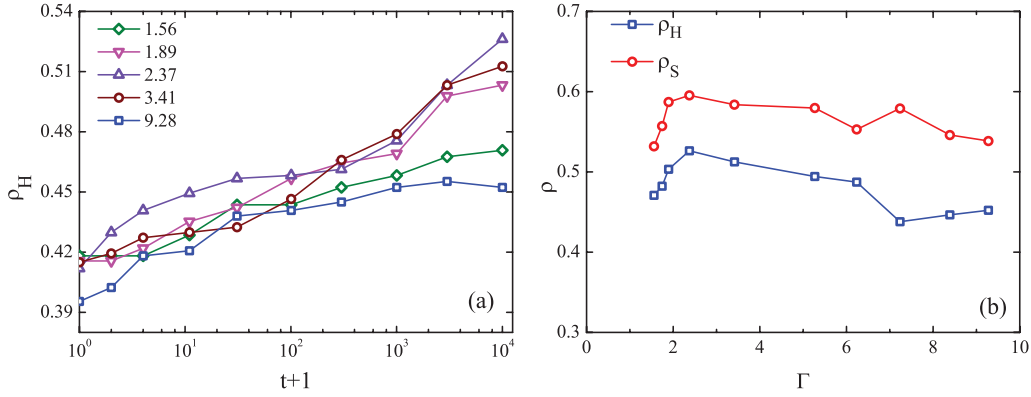
FIG. 2. (Color online) (a) Evolution of the packing density ρ_H as a function of the tapping number for different tapping intensities. (b) Final packing density ρ_H and ρ_S calculated respectively by the total filling height of the packing and from analysis of x-ray tomograms.

the same height. The rods' volume is obtained by integrating all the areas occupied in each tomogram like Fig. 1(d). The corresponding ρ_S is shown in Fig. 2(b). It is obvious that other than a scaling factor, ρ_H and ρ_S show very consistent behavior for the different Γ we measured. We also attempted to fit ρ_H using both Eqs. (1) and (2), and the results are shown in Fig. 3(b). The KWW law yields a consistently better fit as compared to the inverse logarithmic law. So we chose to fit ρ_H using the KWW law for all Γ. The fitting results are shown in Table I. The stretching exponent $\beta = 0.35 \pm 0.05$ is consistent with previous measurements [21,22]. It is worth noting that our experimental configuration is very similar to the Chicago setup [19] in which the strong boundary effect prevents the occurrence of convection. We confirmed the absence of convection by ink labeling several rods to watch their movements under tapping and found no evidence of convection. The good fit of the relaxation dynamics with the KWW law implies a close analogy with thermal glassy behavior [22].

The orientation of each rod within the x-ray tomography reconstructed region can be obtained by an image processing program. As a result, we can directly monitor the structural evolution of the vertical ordering process by calculating the orientational order parameter

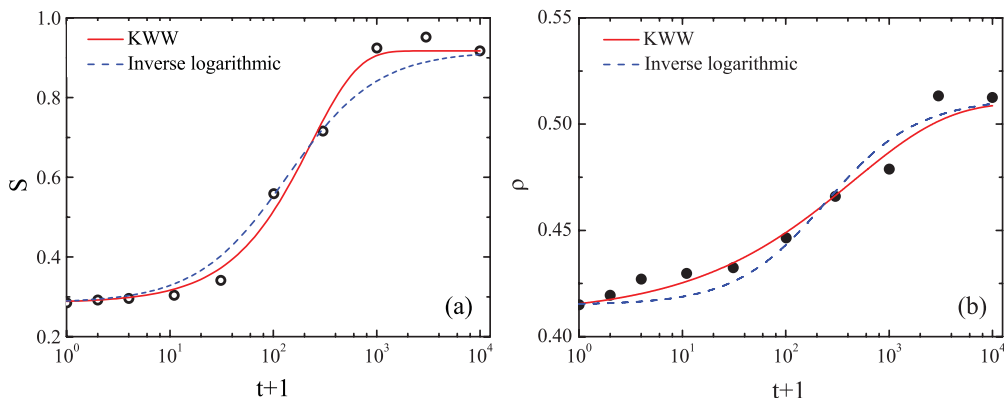$$S = \langle \cos \theta_i \rangle \qquad (3)$$

as function of tap number t, where θ_i is defined as the angle between the long axis of the rod and the vertical axis. θ_i is limited to the range of $0°$–$90°$. S is obtained by averaging over all rods within the reconstructed region. This definition of S is similar to the ordinary nematic order parameter [25–27].

Figure 4 shows the evolution of S as a function of t for different Γ. The ordering process measured by S shows a much clearer trend as compared to ρ_H: S increases slowly when $t < 10^2$ and begins to increase rapidly when $t > 10^2$. At $t = 10^4$, it either continues increasing when Γ is small or saturates at a value when Γ is large. The final orders as measured by S_f at different Γ, which are shown in Fig. 4(b), are consistent with the ρ_H and ρ_S measurements. It suggests that the increase of the packing density is accompanied by an increase of the vertical order. The packing reaches maximum order when $\Gamma = 2.37$. At $\Gamma = 1.56$ or $\Gamma = 1.89$, the order does not saturate after 10^4 times of tapping, which suggests that the time for the system to reach steady state is beyond our experimental time scale.

We also carried out the fitting of the evolution of S using Eqs. (1) and (2) by simply replacing ρ with S and the results are shown in Fig. 3(a); the KWW law also shows consistently better fit than the inverse logarithmic law. In Fig. 4(a), the fitting results for different Γ using the KWW law is

FIG. 3. (Color online) Comparisons of the fitting of (a) orientational order parameter S and (b) packing density ρ_H as a function of the tapping number t at $\Gamma = 3.41$ using both KWW stretched-exponential and inverse logarithmic laws.

TABLE I. Fitting results of the orientational order parameter and packing density using Eq. (2) at different tapping intensities.

Γ	Γ	τ (taps)	β
S	1.89	894 ± 124	0.7 ± 0.1
	2.37	734 ± 62	1.4 ± 0.2
	3.41	232 ± 22	1.0 ± 0.1
	5.26	166 ± 17	1.3 ± 0.2
	8.39	101 ± 24	1.5 ± 0.8
	9.28	129 ± 10	1.3 ± 0.2
ρ	2.37	784 ± 312	0.30 ± 0.05
	3.41	325 ± 82	0.37 ± 0.04

shown, and the corresponding fitting parameters are shown in Table I. One of the important points worth noting is that although S and ρ_H show very similar relaxation time constants τ at the same Γ, their stretching exponents β are clearly different, with β ranging from 0.3 to 0.4 for ρ_H and from 0.9 to 1.6 for S.

IV. BOUNDARY EFFECT ON ORDERING

Our experimental configuration is similar to that of the Chicago group's [19]. In this configuration, it is presumed that the boundary plays an important role in inducing the global order which is absent in the Rennes group's setup [22].

To study the boundary effect upon the ordering process in more detail, we divided the tube's interior into three zones by area proportion 2:1:1 from the border to the center. Rods are grouped into different zones by their center-of-mass locations. Figure 5 shows the fits of S for three zones using the same KWW law as Eq. (2). The corresponding fitting results are shown in Table II. It is evident that the relaxation time τ in general increases from the tube's border to the center, which suggests that the boundary rods order faster than the interior ones. So a phenomenological ordering process happens as follows: the boundary makes the rods which are in contact with it to order vertically first; subsequently, the order gradually propagates into the interior through the rods' intrinsic tendency to align with each other [18].

V. SLOW DYNAMICS

The slow relaxation towards ordering is manifested by the large relaxation time τ for all Γ. In the compaction process, the tapping intensity Γ works like an effective temperature in generating structural rearrangements which lead to compaction. Interestingly, similar to thermal glassy systems, relaxation time τ versus Γ follows an Arrhenius behavior

$$\tau = \tau_0 \exp(\Gamma_0 / \Gamma), \tag{4}$$

where τ_0 and Γ_0 are the characteristic relaxation time and tapping intensity. The fitting results are shown in Fig. 6 with $\tau_0 = 66 \pm 12$(taps) and $\Gamma_0 = 5.1 \pm 0.6$.

The Arrhenius behavior is consistent with our other experimental observations: at small Γ, the ordering time increases rapidly and the packing cannot achieve steady state over our experimental time scale; when Γ is large, the system can reach a steady state since the tapping is energetic enough for the system to explore the phase space.

It has been suggested that the tapping-induced ordering is determined by the diffusion of defect particles and the corresponding ordering time scale is determined by the particles' mobility or random velocity [21,28]. We tried to verify this mechanism by measuring the rods' random motions in the current study. It is worth noting that it is the random and not the overall average motion that drives the rearrangements of the rods which lead to compaction. In the current setup, the random velocity V of each rod is not a directly measurable quantity. Instead, we estimate each rod's V by its relative displacement within the time interval of one tap (1/30 s). Due to the identical nature of the rods, it is difficult to match the same rods after tapping through image processing, especially when Γ is large. To prevent false matches, we coated several rods with thin layers of iodine powders which can induce strong x-ray absorption; these rods are distinguished from the rest on the projection images as shown in Fig. 7. To calculate the relative displacements of these labeled rods during one tap, the tube was rotated along the vertical axis and the projection images were taken at 0° and 90°, from which the three coordinates of the center of mass of the labeled rods can be identified. By taking the projection images at exactly the same two orientations before and after one
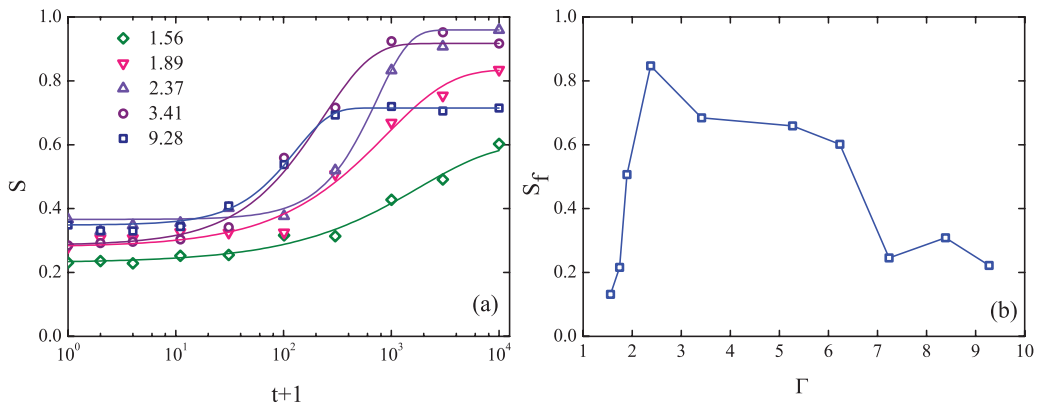

FIG. 4. (Color online) (a) Orientational order parameter S as a function of tapping number t, for different tapping intensities and the corresponding fitting by the KWW law. (b) Final orientational order parameter S_f as a function of vibration intensity.
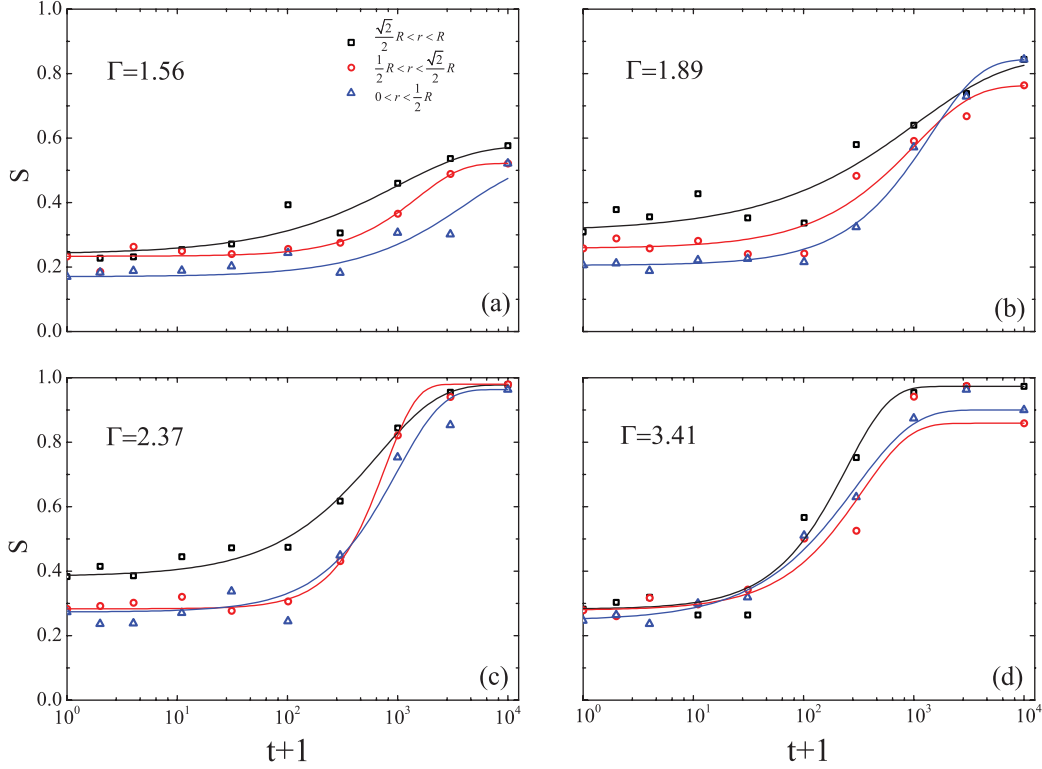
FIG. 5. (Color online) Orientational order parameter S and the corresponding fitting by the KWW law, as a function of tapping number t, for three zones at different tapping intensities (r is the distance from the center, $\sqrt{2}R/2 < r < R$ represents the zone near the boundary, $R/2 < r < \sqrt{2}R/2$ represents the middle zone, and $0 < r < R/2$ represents the central zone).

tap, the displacements of the center of mass of labeled rods along all three Cartesian coordinates can be calculated. The measurements were repeated around ten times at each Γ. In the current experiment, we focus on the initial random velocities of the rods during the first tap after preparation. So the tube was emptied and the packing was prepared freshly after each measurement.

In Fig. 8, the histograms show the distributions of V measured at different Γ. It is obvious that there exists a large dispersion of V for all Γ. There is a large dispersion of the heterogeneous dynamics in colloidal and granular systems in which the relaxation dynamics is mostly determined by a few very fast-moving particles [29,30]. We can calculate the mean random velocity $\langle V \rangle$ of all rods for different Γ by taking a simple average of all measurements. The corresponding $\langle V \rangle$ as a function of Γ is shown in Fig. 9. Despite the large dispersion in V, $\langle V \rangle$ increases as Γ increases. It is

interesting to note, if we can assume the ordering process is a defect-controlled simple diffusion process [21,28], we can use $\langle V \rangle$ to estimate the average length scale a rod can diffuse over the relaxation time τ for different Γ. It turns out that this length scale is about two to three times the length of the rod for all Γ, although this reasoning is an oversimplification since obviously the ordering process is controlled by both translational and rotational degrees of freedom and there is no guarantee of energy equipartition among them. However, the
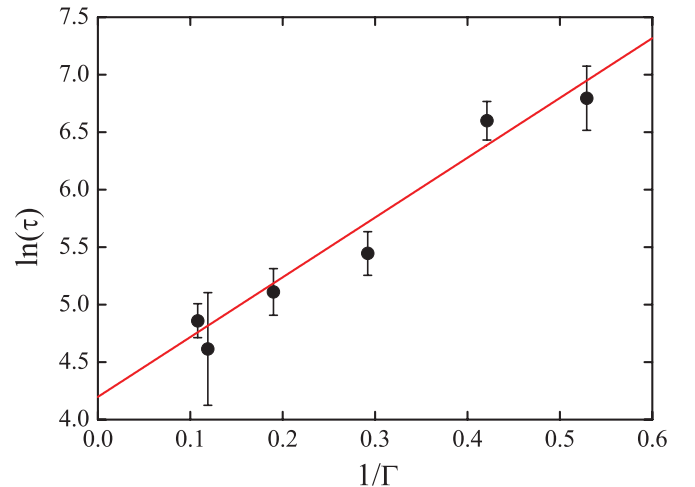
TABLE II. Fitting results of the relaxation time of three zones for different tapping intensities using Eq. (2). $R = 5$ mm is the inner radius of the container.

Γ	τ (taps)		
	$\sqrt{2}R/2 < r < R$	$R/2 < r < \sqrt{2}R/2$	$0 < r < R/2$
1.55	996 ± 154	1522 ± 333	4068 ± 474
1.89	1076 ± 775	1023 ± 246	1418 ± 189
2.37	661 ± 94	774 ± 42	992 ± 138
3.41	245 ± 105	337 ± 129	296 ± 54

FIG. 6. (Color online) Fitting of the relaxation time τ as a function of the inverse tapping intensity to an Arrhenius behavior as in Eq. (4).
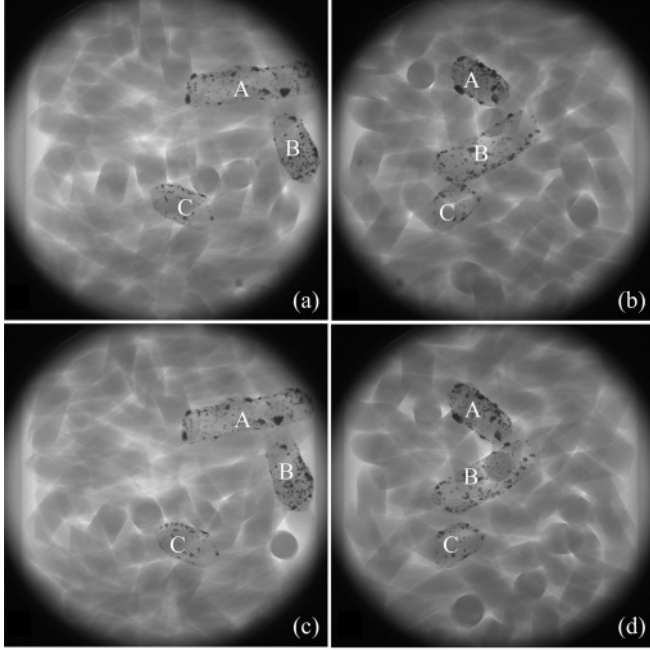
FIG. 7. X-ray projection images of the iodine-labeled rods taken at two perpendicular orientations before and after one tap at $\Gamma = 2.37$. [(a),(b)] $0°$ and $90°$ before tapping. [(c),(d)] $0°$ and $90°$ after tapping.

presumption of a simple diffusion process [28] is compatible with our experimental observations.

We also calculated the mean random kinetic energy of the rods using

$$E_k = \langle mV^2/2 \rangle, \qquad (5)$$

where m is the mass of the rod. E_k is only around several percent of the gravitational potential energy $mgL/2$ of a rod when it aligns vertically [31]. The overall average kinetic energy gained for each rod from one tap is

$$U_{\exp} = mA^2\omega^2/2 = m\Gamma^2 g/2\omega^2, \qquad (6)$$

where ω is the angular frequency of the tapping. Comparing the random kinetic energy with the overall kinetic energy we arrive at $E_k/U_{\exp} = 0.042$. So only a very small fraction of the input energy is turned into the random motion of the rods.

VI. COORDINATION NUMBER

The coordination number and the associated free volume of each particle were essential in the statistical description of granular packings [32,33]. In the current study, we analyzed the average coordination number $\langle Z \rangle$ by directly counting the contacting neighbors through a direct structure analysis.

The coordination number in spherical granular packings has been extensively studied [32]. In spherical packings, using an isostatic argument, $\langle Z \rangle$ equals $2N$ for frictionless particles and $N + 1$ for frictional particles, where N is the degree of freedom. A similar reasoning has been applied to rods [34]: the corresponding $\langle Z \rangle$ equals 10 in the frictionless case and 6 in the frictional case, in which we have assumed that $N = 5$ for rods.

The coordination number Z for the rod packing has been measured previously following the similar technique by Bernal
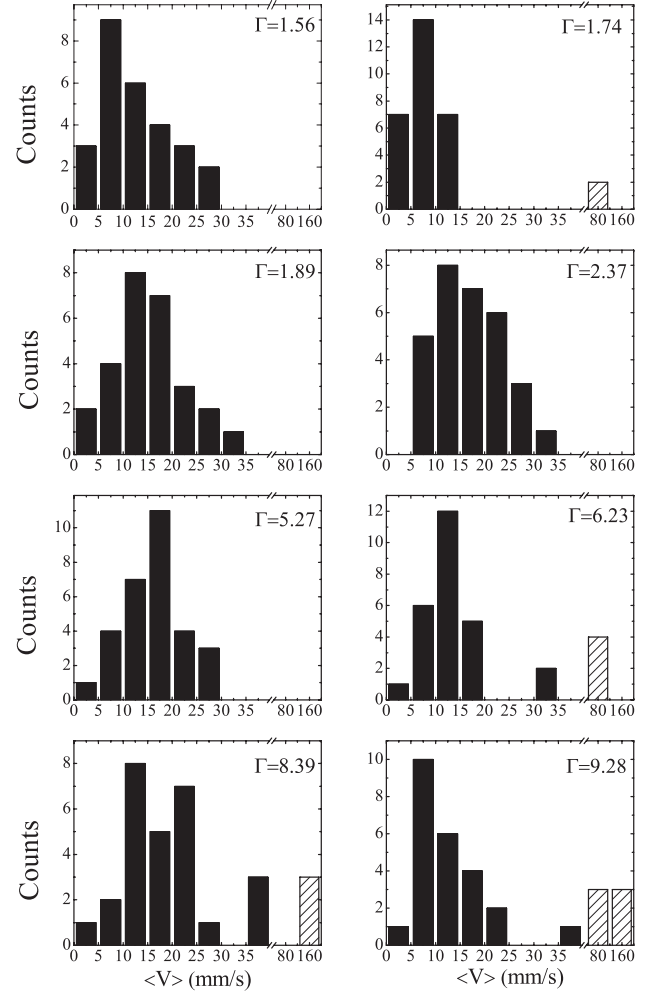

FIG. 8. Histograms of the distributions of random velocities of labeled rods for different Γ.

[35,36]. In the current study, we directly obtain Z and its distribution using noninvasive structural information alone.
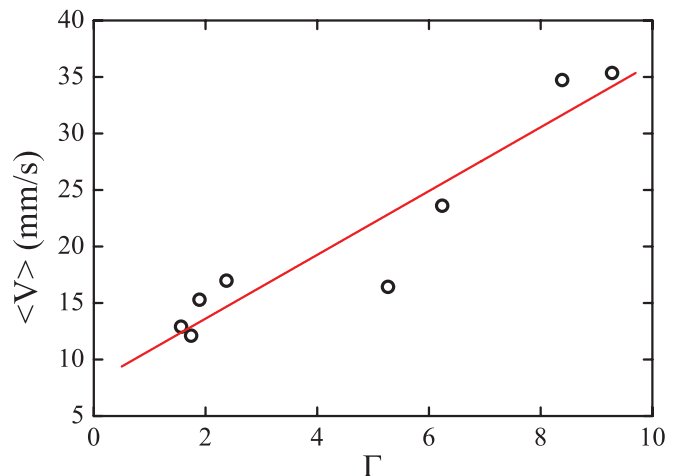

FIG. 9. (Color online) Mean random velocity $\langle V \rangle$ as a function of vibration intensity Γ.
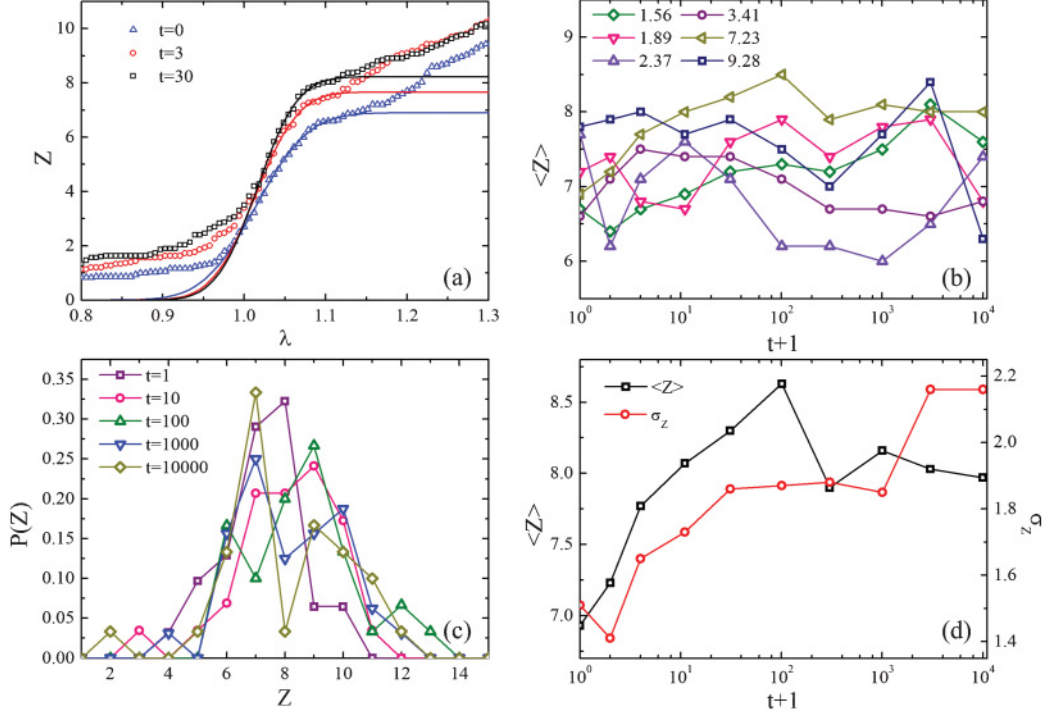
FIG. 10. (Color online) (a) Coordination number Z as a function of the normalized minimum distance parameter λ for several tapping numbers at $\Gamma = 7.23$. Solid lines are the fitting results using Eq. (7). (b) Average coordination number $\langle Z \rangle$ as a function of the tapping number for different tapping intensities. (c) Probability distribution functions of coordination number Z. (d) Corresponding averages and variances as a function of the tapping number at $\Gamma = 7.23$.

Through image analysis, the center of mass and the orientation of all rods can be extracted. Two rods are considered contacting neighbors if the minimum distance r between their finite-length centerlines equals their diameter d. In practice, this criteria is very difficult to implement due to the uncertainty in the determination of the rods' center of mass, orientation, and a size distribution of the rods. We adopted a similar technique from a previous study for the determination of Z [9]: First, the minimum distance r between a rod and any other rod has been calculated, and it is normalized by d in getting the normalized minimum distance parameter $\lambda = r/d$. Two rods are considered contacting neighbors if their normalized distance is smaller than some value of λ. In the ideal case, Z as a function of λ will show an abrupt jump from zero at $\lambda = 1$ to the ideal coordination number value and then increase gradually as λ increases. In reality, Z displays a much more gradual increase around $\lambda = 1$ as shown in Fig. 10(a). Therefore, in practice, a small Gaussian distribution of λ has been assumed. The resulting Z versus λ can then be well fitted by a complementary error function assuming the form

$$Z(\lambda) = \frac{\langle Z \rangle}{\sqrt{2\pi}} \int_{(d_m - \lambda d)/\xi}^{\infty} \exp\left(-\frac{t^2}{2}\right) dt, \qquad (7)$$

where ξ is the variance of the Gaussian distribution and d_m is the fitted actual average minimum distance between rods. The fitting results for several tapping numbers at $\Gamma = 7.23$ are shown in Fig. 10(a). The average coordination number $\langle Z \rangle$ and the probability distribution function of Z can also be obtained for the rods within our reconstructed image region. One thing to note is that in the above analysis, we have been

very careful by only using rods which have no contacts with the tube boundary and at the same time are away from the top and bottom of the imaging window. As shown in Fig. 10(b), the average coordination number $\langle Z \rangle$ spans a range from 6 to 8 as function of t for different Γ. There is a certain increasing trend of $\langle Z \rangle$ as t increases. However, due to the small number of rods in our imaging window, this trend is not conclusive. An average coordination number value from 6 to 8 is consistent with a frictional rod packing with medium aspect ratios [36]. Figure 10(c) shows the probability distribution functions of the coordination number Z for different tapping numbers t at $\Gamma = 7.23$. The results of a simple Gaussian fit are shown in Fig. 10(d) with the corresponding standard deviation σ_Z lying in the range from 1.4 to 2.2.

VII. CONCLUSION

In conclusion, we have carried out a preliminary study of the compaction process of rods under tapping using x-ray tomography. We directly measured the evolution of the orientational order parameter, with the local and global packing densities as functions of the tapping number for different tapping intensities. The slow relaxation dynamics can be well fitted using a KWW-type stretched-exponential law. The corresponding relaxation time vs tapping intensity follows an Arrhenius behavior. After measuring the mean velocity of the rods gained from one tap, we found that the ordering process can be well described by a diffusive process, with the tube boundary rods order faster than the interior ones. The average coordination number has also been measured, which spans a range from 6 to 8.

[1] P. Richard, M. Nicodemi, R. Delannay, P. Ribiere, and D. Bideau, Nat. Mater. **4**, 121 (2005).

[2] A. J. Liu and S. R. Nagel, Nature (London) **396**, 21 (1998).

[3] S. F. Edwards and C. C. Mounfield, Physica A **210**, 290 (1994).

[4] T. Boutreux and P. G. de Gennes, Physica A **244**, 279 (1997).

[5] E. Ben-Naim, J. B. Knight, E. R. Nowak, H. M. Jaeger, and S. R. Nagel, Physica D **123**, 380 (1998).

[6] M. Nicodemi, A. Coniglio, and H. J. Herrmann, Phys. Rev. E **55**, 3962 (1997).

[7] A. Mehta, G. C. Barker, and J.-M. Luck. Phys. Today **62**, 40 (2009).

[8] P. Philippe and D. Bideau, Phys. Rev. E **63**, 051304 (2001).

[9] T. Aste, M. Saadatfar, and T. J. Senden, Phys. Rev. E **71**, 061302 (2005).

[10] W. Zhang, K. E. Thompson, A. H. Reed, and L. Beenken, Chem. Eng. Sci. **61**, 8060 (2006).

[11] M. Tsukahara, S. Mitrovic, V. Gajdosik, G. Margaritondo, L. Pournin, M. Ramaioli, D. Sage, Y. Hwu, M. Unser, and Th. M. Liebling, Phys. Rev. E **77**, 061306 (2008).

[12] G. T. Seidler, G. Martinez, L. H. Seeley, K. H. Kim, E. A. Behne, S. Zaranek, B. D. Chapman, S. M. Heald, and D. L. Brewe, Phys. Rev. E **62**, 8175 (2000).

[13] O. Pouliquen, M. Belzons, and M. Nicolas, Phys. Rev. Lett. **91**, 014301 (2003).

[14] L. Berthier and G. Biroli, Rev. Mod. Phys. **83**, 587 (2011).

[15] P. Philippe and D. Bideau, Europhys. Lett. **60**, 677 (2002).

[16] J. B. Knight, C. G. Fandrich, C. N. Lau, H. M. Jaeger, and S. R. Nagel, Phys. Rev. E **51**, 3957 (1995).

[17] A. Donev, I. Cisse, D. Sachs, E. A. Variano, F. H. Stillinger, R. Connelly, S. Torquato, and P. M. Chaikin, Science **303**, 990 (2004).

[18] L. Onsager, Ann. N.Y. Acad. Sci. **51**, 627 (1949).

[19] F. X. Villarruel, B. E. Lauderdale, D. M. Mueth, H. M. Jaeger, and S. R. Nagel, Phys. Rev. E **61**, 6914 (2000).

[20] P. Ribiere, P. Richard, D. Bideau, and R. Delannay, Eur. Phys. J. E **16**, 415 (2005).

[21] G. Lumay and N. Vandewalle, Phys. Rev. E **74**, 021301 (2006).

[22] P. Ribiere, P. Richard, D. Bideau, and Delannay, Eur. Phys. J. E **16**, 415 (2005).

[23] G. Lumay and N. Vandewalle, Phys. Rev. Lett. **95**, 205502 (2005).

[24] Y. Cao, B. Chakrabortty, G. C. Barker, A. Mehta, and Y. Wang, arxiv:1112.3146v1.

[25] P. J. Steinhardt, D. R. Nelson, and M. Ronchetti, Phys. Rev. B **28**, 784 (1983).

[26] B. J. Buchalter and R. M. Bradley, Phys. Rev. A **46**, 3046 (1992).

[27] J. Galanis, D. Harries, D. Sackett, W. Losert, and R. Nossal, Phys. Rev. Lett. **96**, 028002 (2006).

[28] K. L. Gavrilov, Phys. Rev. E **58**, 2107 (1998).

[29] E. R. Weeks, J. C. Crocker, A. C. Levitt, A. Schofield, and D. A. Weitz, Science **287**, 627 (2000).

[30] A. S. Keys, A. R. Abate, S. C. Glotzer, and D. J. Durian, Nat. Phys. **3**, 260 (2007).

[31] M. Ramaioli, L. Pournin, and Th. M. Liebling, Phys. Rev. E **76**, 021304 (2007).

[32] P. Richard, P. Philippe, F. Barbe, S. Bourles, X. Thibault, and D. Bideau, Phys. Rev. E **68**, 020301 (2003).

[33] C. Song, P. Wang, and H. A. Makse, Nature (London) **453**, 629 (2008).

[34] A. P. Philipse, Langmuir **12**, 1127 (1996).

[35] S. Torquato and F. H. Stillinger, Rev. Mod. Phys. **82**, 2633 (2010).

[36] J. Blouwolff and S. Fraden, Europhys. Lett. **76**, 1095 (2006).